

Doubly differential cross section of secondary electrons ejected from gases by electron impact: 50–400 eV on CO₂

T. W. Shyn and W. E. Sharp

Space Physics Research Laboratory, Department of Atmospheric and Oceanic Science, University of Michigan, Ann Arbor, Michigan 48109

(Received 12 February 1979)

Doubly differential cross sections of secondary electrons ejected from CO₂ by electron impact have been measured by means of a crossed-beam method. The incident energies used were 50, 100, 200, and 400 eV. The energy range and angular range of secondary electrons measured were from one-half of the difference between incident energy and ionization potential to 1.0 eV and from 12 to 156°, respectively. The present results agree with the results of Rapp and Englander-Golden for the total ionization cross sections and with that of Opal *et al.* for the singly differential cross sections. The doubly differential cross sections show larger values at extreme angles and smaller values near 90° than those of Opal *et al.*

I. INTRODUCTION

Ionization of atoms and molecules by electron impact is one of the most important physical processes in atomic physics and the ionization cross sections are very important quantities used in other areas of study (planetary atmospheres, plasma physics, radiation physics, etc.).

Ionization of CO₂ by electron impact has been studied by a few authors, primarily to find the total and dissociative ionization cross sections. Rapp and Englander-Golden¹ have measured the total cross sections for ionization including dissociative ionization (production of O⁺, C⁺, and CO⁺). They have used an ionization tube with an incident electron beam in the energy from threshold to 1000 eV. Crowe and McConkey² reported the angular distribution of CO₂⁺ and dissociative ions produced from CO₂ by electron impact for incident energies from threshold to 300 eV. The angular range in these measurements were between 45 and 135°. Märk and Hille³ have measured the single and double ionization cross section of CO₂ by electron impact from threshold up to 180 eV. Other studies reporting partial cross section measurements for the various ions from CO₂ by electron impact include those of Peresse and Tuffin⁴ and of Adamczyk *et al.*⁵

The only measurement of doubly differential cross sections (DDCS) ($d^2\sigma/dE d\Omega$ in angle and energy) of secondary electrons ejected from CO₂, however, has been made by Opal *et al.*⁶ An incident energy of 500 eV was used. The energy range and angular range of the secondary electrons measured were from 30 to 150° and from 4 to 205 eV, respectively.

This paper, which is the second in a series presenting results of an extensive study⁷ of secondary electrons ejected from atmospheric gases by

electron impact, presents the results of an experimental study in which the DDCS of secondary electrons ejected from CO₂ by electron impact have been measured using a crossed-beam method. Incident energies of 50, 100, 200, and 400 eV have been used. The energy and angular range of the secondary electrons measured were from one-half of the difference between the incident energy and ionization potential down to 1.0 eV and from 12 to 156°, respectively. The present results include all the dissociative ionization processes in addition to the direction ionization of CO₂ (CO₂⁺, CO₂²⁺, etc.).

II. APPARATUS AND PROCEDURE

The apparatus used for the present measurements is the same as that used previously⁷ for the measurements of DDCS of secondary electrons ejected from He and detailed descriptions can be found elsewhere.⁷⁻⁹ The pumping speed for CO₂ was improved by utilizing a cryogenic pump (liquid nitrogen) which reduced the background pressure considerably. A brief description of the apparatus is as follows: a rotatable electron beam interacts at 90° with a neutral beam collimated by a fused capillary array. Secondary electrons ejected from the neutral beam are detected in a detector system after energy analysis. The typical electron beam current from the electron beam monochromator is 10⁻⁷ A with an energy half-width of 0.2 eV and a divergence angle of ±2°. The detector system has an acceptance angle of ±4°. The resultant angular resolution of the present experiment is estimated to be ±4°.

The vacuum enclosure is pumped by a turbomolecular pump and a cryogenic pump down to pressure of 10⁻⁹ Torr without baking the system. With the neutral beam of CO₂ on, the background

pressure rose to 1×10^{-6} Torr and the density of the beam in the interaction region was estimated to be greater than the background density by a factor of 30. At the background pressure of 1×10^{-6} Torr the attenuation of ejected electrons from the interaction region to the detector, mainly due to the elastic scattering, has been calculated to be less than $10^{-2}\%$.

The magnetic fields in the plane of measurement are compensated by three sets of Helmholtz coils and have been measured to be less than 20 mG in all directions.

The absolute energy scale was determined frequently to within 0.05 eV using the He resonance at 19.35 eV.

The ejected electrons were detected by the detector system without the use of any electron lens system (lens systems were turned off) in order to ensure a constant transmission of the analyzer against energy. The transmission of the analyzer has been measured to be constant within 5% down to an electron energy of 2.0 eV.

The procedure used for the present measurements was the same as the previous measurement⁷ of He. The collimated beam of CO₂ was turned on and at a given incident energy the signal was integrated for 10 sec at each scattering angle from 12 to 156° in 12° increments and secondary electron energy. The measurements were repeated with the neutral beam off to obtain the background count. The difference between the two signals is the DDCS of secondary electrons ejected from the CO₂ beam.

The correction of the final data for volume scattering effects (effective path length) which come from the background density (static gas target) has been made. At 90° (the minimum contribution), this component is $3 \pm 1\%$ of the total signal.

III. EXPERIMENTAL RESULTS

The DDCS of secondary electrons were measured at four incident energies, 50, 100, 200, and 400 eV.

Table I shows a typical signal-background ratio of data points for low secondary energies. The worst ratio was $\frac{1}{3}$ at 1 eV secondary energy with incident energies at 200 and 400 eV as expected. The range of the ratio for higher secondary energies (>5 eV) was from $\frac{3}{4}$ to $\frac{15}{4}$. Six sets of data from the low-energy secondary electrons (<5 eV) and four sets for the rest have been taken and averaged to produce final results. The results have been calibrated among themselves (among secondary electron energies and among incident energies) and have been placed on an absolute scale using the elastic scattering cross sections

TABLE I. Signal-background ratio of data points for low secondary energies.

E_s^b (eV) \ E_i^a (eV)	50	100	200	400
1	1/2	1/1	1/3	1/3
2	1/1	2/1	1/1	1/1
3	2/1	3/2	3/2	1/1
4	3/1	3/2	3/2	1/1
5	4/1	3/1	2/1	3/2

^a E_i = incident energy.

^b E_s = secondary energy.

of CO₂ at 50 eV measured by Shyn *et al.*⁹

The statistical uncertainty of the data points were less than 4% except for low secondary energies and at small angle (12°). The largest statistical uncertainty of data points at 12° (400-eV incident energy) was estimated to be 20% approximately, because of the higher background counts compared to all other angles. There was uncertainty of 10% in the calibration of the inter-secondary electron energies and 5% in the inter-incident energy calibrations. In the normalization process to the elastic cross section of CO₂ at 50 eV, an uncertainty has been estimated to be less than 5%. The volume correction had a 3% uncertainty. In addition to these statistical uncertainties, there is a systematic uncertainty in the normalization process of the elastic cross-section measurements of CO₂ to that of He which contributed 10% (this has been reported in the previous paper⁹). The resultant uncertainty of the present results is estimated to be 17% except for low secondary energies. The largest resultant uncertainty is less than 26% (at 1-eV secondary energy and 400-eV incident).

The final results are shown in Tables II–V for the four incident energies, respectively. As noted previously, the present results contain all the contributions from the dissociative ionizations (production of C⁺, O⁺, and CO⁺) in addition to the direct ionizations (CO₂⁺, CO₂²⁺, etc.).

Figure 1 shows a three-dimensional-perspective diagram of secondary electrons ejected from CO₂ by electron impact at 50-eV incident energy. Below 6 eV, the distribution is isotropic with the exception of a strong forward peak at angles less than 60°. Above 6 eV, the isotropy begins to disappear with backward scattering becoming more probable relative to the scattering at 90°. At 18 eV, the forward and backward scattering are nearly symmetrical about 90°.

The forward peak did not come from the elastic scattering even if the incident electron beam contained some components of low-energy electrons

TABLE II. DDGS ($d^2\sigma/d\Omega dE$) of secondary electrons ejected from CO₂ by 50-eV electron impact (in units of 10^{-49} cm²/sr eV). (The numbers in parentheses represent extrapolated data points.)

E_s (eV)	θ°	12	24	36	48	60	72	84	96	108	120	132	144	156	168	$\Delta\sigma/\Delta E$ (10^{-47} cm ² /eV)
1.0		144.2	37.5	21.9	9.3	6.8	7.1	6.8	6.8	7.9	7.4	8.5	9.6	(9.3)	(9.0)	1.608
2.0		139.8	50.0	28.3	17.0	14.2	14.7	15.2	15.6	15.6	16.3	17.8	17.3	(15.3)	(13.2)	2.547
3.0		109.7	43.6	23.2	17.9	13.8	14.4	14.7	14.7	15.0	15.4	16.0	15.2	13.3	(11.9)	2.337
4.0		60.5	18.7	15.5	13.8	10.8	11.3	12.2	11.8	11.5	12.3	11.7	11.4	11.0	(9.9)	1.657
5.0		48.0	22.1	13.4	12.4	9.6	9.7	10.0	10.2	10.1	10.0	11.2	11.5	11.4	(11.4)	1.460
6.0		27.9	15.6	12.8	11.0	9.2	8.8	8.9	9.2	9.5	10.3	11.6	12.1	11.8	(11.5)	1.351
8.0		30.9	17.0	12.0	10.0	8.2	8.1	7.9	8.0	8.4	9.0	10.1	11.0	13.2	(14.7)	1.279
10.0		40.8	16.5	12.4	10.0	8.3	7.5	6.9	6.8	7.1	8.4	9.7	11.3	13.9	(16.6)	1.250
12.0		55.9	14.5	10.5	8.5	7.4	6.2	5.9	5.1	5.8	6.5	8.1	10.3	13.7	(17.0)	1.126
15.0		37.2	15.4	10.4	7.9	6.0	5.2	4.7	4.2	4.3	5.5	7.6	9.0	11.6	(14.2)	0.961
18.1		38.8	16.9	9.3	6.4	5.2	4.3	3.7	3.7	4.0	4.7	5.8	7.4	10.0	(12.6)	0.849

TABLE III. DDGS ($d^2\sigma/d\Omega dE$) of secondary electrons ejected from CO₂ by 100-eV electron impact (in units of 10^{-49} cm²/sr eV). (The numbers in parentheses represent extrapolated data points.)

E_s (eV)	θ°	12	24	36	48	60	72	84	96	108	120	132	144	156	168	$\Delta\sigma/\Delta E$ (10^{-48} cm ² /eV)
1.0		242.9	55.1	23.1	12.2	10.7	8.2	8.7	8.9	8.7	9.8	10.3	12.4	13.3	(14.7)	22.38
2.0		152.0	40.7	24.2	18.3	14.5	14.4	15.5	15.7	16.5	19.5	21.1	22.1	24.6	(27.2)	27.62
3.0		123.0	48.1	29.9	20.2	15.1	14.5	14.4	13.8	14.8	17.8	18.3	19.5	23.1	(27.1)	26.62
4.0		90.4	34.9	21.7	16.8	11.4	11.9	11.8	11.6	11.7	11.7	12.7	13.4	13.8	(17.0)	19.94
5.0		65.5	27.4	17.4	14.0	10.9	10.9	11.0	10.9	11.1	11.7	12.5	12.6	13.2	(14.1)	17.53
6.0		54.4	21.0	15.1	12.5	10.3	9.6	9.6	9.6	10.0	10.4	11.3	12.3	13.1	(14.0)	19.40
8.0		33.4	17.0	12.5	10.6	8.9	8.2	7.9	7.9	8.1	8.6	9.6	10.7	13.2	(14.9)	12.85
10.0		26.1	12.7	10.0	8.3	7.2	6.7	6.4	6.2	6.4	6.6	7.6	8.7	10.3	(11.9)	10.12
12.0		20.8	11.0	8.6	7.4	6.3	5.6	5.3	5.1	5.1	5.4	6.2	7.4	9.3	(10.6)	8.55
15.0		20.1	14.4	9.5	7.5	5.3	4.6	4.2	4.0	4.5	4.9	6.3	7.8	7.8	(9.3)	8.18
20.0		17.6	9.0	6.5	5.6	4.6	4.0	3.5	3.3	3.3	3.7	4.3	4.5	6.5	(8.1)	6.18
25.0		10.8	6.2	4.6	3.8	3.1	2.7	2.3	2.1	2.2	2.4	3.0	3.7	4.7	(5.7)	4.18
30.0		8.9	5.1	3.7	3.0	2.4	1.9	1.7	1.4	1.5	1.8	2.2	2.9	3.8	(4.8)	3.14
35.0		9.9	5.6	3.7	2.7	2.0	1.5	1.3	1.1	1.2	1.5	1.9	2.7	3.6	(4.6)	2.87
40.0		11.9	6.1	3.6	2.4	1.7	1.3	1.1	0.91	0.99	1.2	1.7	2.0	3.2	(4.3)	2.65
43.1		13.9	6.5	3.5	2.4	1.6	1.1	0.91	0.76	0.89	1.1	1.5	2.1	3.0	(4.0)	2.61

TABLE IV. DDCS ($d^2\sigma/d\Omega dE$) of secondary electrons ejected from CO₂ by 200-eV electron impact (in units of 10⁻²⁰ cm²/sr eV). (The numbers in parentheses represent extrapolated data points.)

E_s (eV)	θ°	12	24	36	48	60	72	84	96	108	120	132	144	156	168	$\Delta\sigma/\Delta E$ (10 ⁻¹⁸ cm ² /eV)
1.0		2602.4	567.5	158.8	75.8	64.4	41.3	27.7	23.0	27.6	36.8	32.2	29.9	39.1	(50.6)	15.66
2.0		1672.0	508.0	265.2	122.0	85.5	77.7	72.4	80.1	87.9	94.9	105.0	107.3	101.7	(97.2)	19.29
3.0		1024.4	324.1	234.2	128.5	103.5	81.8	99.9	89.6	92.8	98.5	99.9	105.6	127.1	(148.5)	20.12
4.0		876.5	320.6	212.2	151.0	103.1	93.6	94.9	98.7	105.3	106.9	125.2	108.7	120.6	(132.6)	17.52
5.0		576.8	217.4	168.3	122.4	96.5	86.7	87.6	86.3	91.4	93.4	96.1	92.6	104.0	(115.8)	14.44
6.0		465.5	236.5	135.5	102.8	86.4	78.0	79.5	79.2	81.3	84.0	86.7	87.0	93.9	(100.8)	12.90
8.0		347.9	131.9	118.6	89.1	75.6	69.8	67.7	67.3	69.2	67.6	71.2	79.3	89.7	(100.2)	10.64
10.0		269.4	117.3	91.4	75.3	64.7	59.1	56.3	54.0	54.3	55.0	59.8	64.7	77.3	(89.9)	8.76
12.0		184.1	90.3	64.2	66.0	57.5	52.9	48.1	47.3	43.9	47.6	50.1	56.8	68.6	(80.2)	7.39
15.0		128.1	69.0	59.4	52.6	47.0	42.6	39.8	36.8	35.6	36.1	38.6	43.2	51.8	(60.4)	5.77
20.0		101.8	62.2	50.5	42.3	36.1	33.4	29.7	27.0	26.0	25.8	27.1	30.9	37.8	(44.2)	4.46
25.0		94.9	60.5	36.3	28.1	22.7	18.3	17.8	15.6	15.0	16.0	18.0	23.0	29.6	(36.3)	3.22
30.0		69.6	42.6	29.0	23.9	19.8	16.6	13.5	12.8	12.4	12.8	15.1	19.5	24.5	(29.7)	2.52
35.0		50.5	26.2	20.4	17.7	15.5	13.0	10.7	9.12	8.66	9.27	10.6	13.2	17.3	(21.4)	1.77
40.0		41.9	21.4	16.3	14.0	11.5	10.1	7.38	6.70	6.15	6.77	7.44	9.80	11.9	(13.9)	1.32
50.0		22.6	12.8	10.8	9.27	7.57	5.87	4.66	3.43	3.39	3.86	4.26	5.75	7.68	(9.50)	0.81
65.0		24.5	13.0	7.39	6.58	4.66	3.18	2.72	2.01	2.13	2.04	2.80	3.90	4.69	(5.47)	0.56
80.0		25.8	15.0	8.89	5.53	3.66	2.30	1.63	1.50	1.45	1.70	2.24	3.02	4.18	(5.71)	0.49
93.1		31.9	16.2	7.83	5.02	2.72	1.57	1.47	0.87	1.03	1.30	1.50	1.98	3.06	(4.16)	0.45

TABLE V. DDOS ($d^2/d\Omega dE$) of secondary electrons ejected from CO₂ by 400-eV electron impact (in units of 10^{-20} cm²/sr eV). (The numbers in parentheses represent extrapolated data points.)

E_s (eV)	θ°	12	24	36	48	60	72	84	96	108	120	132	144	156	168	$\Delta\sigma/\Delta E$ (10^{-18} cm ² /eV)
1.0		2055.3	392.1	128.5	75.2	43.6	36.3	31.8	29.1	26.7	26.7	24.2	21.7	(18.1)	(14.5)	12.66
2.0		1727.2	490.7	242.4	121.3	67.1	59.7	52.3	48.5	46.7	46.7	42.9	39.2	(34.0)	(28.3)	12.50
3.0		1206.0	411.1	222.5	118.0	73.3	67.8	69.2	66.5	59.7	59.7	52.9	40.7	36.3	(31.2)	14.44
4.0		727.5	284.8	178.8	94.7	65.3	62.0	58.1	59.6	57.9	57.9	51.4	46.5	46.5	(35.1)	11.43
5.0		514.8	191.9	159.1	94.9	70.2	62.4	62.9	62.9	60.8	58.8	55.8	46.1	42.8	(40.7)	10.51
6.0		414.9	200.4	138.9	80.3	62.9	56.8	55.6	56.3	53.0	53.0	47.0	40.8	39.4	(39.9)	9.32
8.0		250.3	128.5	105.6	69.0	53.4	51.5	49.0	48.7	48.0	49.7	44.3	41.0	46.3	(51.1)	7.70
10.0		194.4	91.0	77.9	57.3	48.5	44.4	42.5	40.7	38.9	38.5	37.4	35.9	42.0	(48.5)	6.30
12.0		149.2	86.3	65.1	50.3	44.1	39.4	38.1	36.1	34.2	32.1	31.5	31.9	34.4	(37.1)	5.47
15.0		92.9	63.1	51.7	44.9	37.8	35.0	32.8	30.0	27.8	27.0	26.4	26.7	32.8	(35.1)	4.52
20.0		61.3	42.7	35.6	32.6	28.9	26.3	24.9	22.1	20.3	19.2	18.5	18.8	22.3	(26.0)	3.26
25.0		42.9	29.2	25.2	23.5	21.3	20.1	18.2	16.3	14.8	13.7	13.5	14.4	17.4	(20.4)	2.38
30.0		31.1	25.2	17.2	18.0	16.9	15.3	13.4	11.7	10.1	9.58	9.65	10.9	13.2	(15.6)	1.76
35.0		22.9	17.6	13.8	14.1	12.9	11.6	9.96	8.59	7.38	6.86	7.05	8.06	10.2	(12.5)	1.32
40.0		20.1	12.8	11.1	11.2	10.6	9.04	7.83	6.32	5.42	4.97	5.42	6.20	7.74	(8.74)	1.04
50.0		16.4	10.2	7.34	7.90	7.16	6.17	5.08	3.89	3.31	3.31	3.35	3.76	4.88	(6.04)	0.687
65.0		9.20	5.16	4.67	5.17	4.85	3.82	2.77	2.07	1.79	1.71	1.85	2.21	2.89	(3.64)	0.401
80.0		6.82	4.45	3.06	3.70	3.23	2.49	1.71	1.25	1.03	1.09	1.16	1.45	1.84	(2.22)	0.277
100.0		6.22	3.31	2.45	2.87	2.40	1.54	1.04	0.66	0.63	0.65	0.65	0.89	1.03	(1.16)	0.188
120.0		4.38	2.68	2.12	2.34	1.66	1.05	0.60	0.50	0.42	0.38	0.50	0.58	0.73	(0.91)	0.137
140.0		4.81	2.43	2.15	2.11	1.54	0.90	0.53	0.47	0.45	0.42	0.47	0.56	0.73	(0.86)	0.131
160.0		6.16	2.84	2.36	1.95	1.27	0.81	0.56	0.42	0.39	0.36	0.40	0.49	0.61	(0.71)	0.129
180.0		7.22	3.21	2.43	1.28	1.03	0.67	0.48	0.40	0.33	0.36	0.39	0.41	0.50	(0.61)	0.123
193.1		7.20	3.54	2.68	1.45	0.91	0.59	0.43	0.37	0.33	0.33	0.36	0.38	0.49	(0.64)	0.120

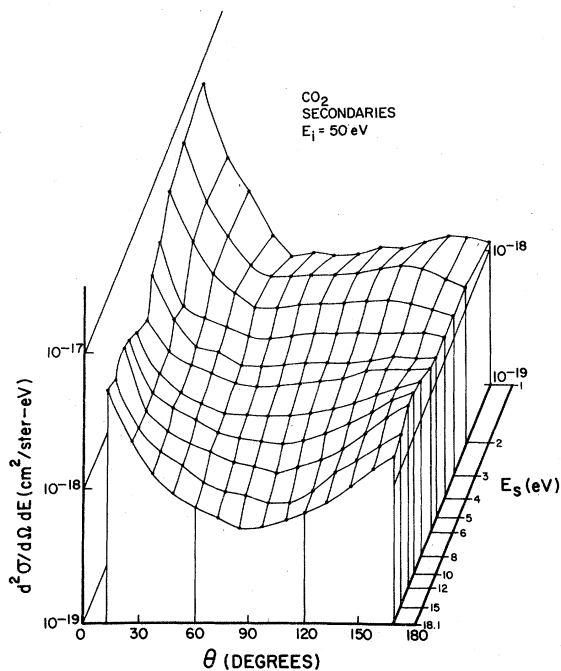


FIG. 1. Three-dimensional-perspective diagram of secondary electrons ejected from CO_2 by 50-eV electron impact.

because, as shown in the previous paper⁹ of CO_2 elastic scattering measurements, the angular distributions of elastic scattering cross sections at low energies (<5 eV) do not have a strong forward peak comparable to the forward peak in the double differential cross section in the present measurement. Also, as mentioned in the recent paper⁷ for He secondary electron measurements, the intensity of low-energy electrons, including the surface secondary electrons produced by the incident electrons from the metal surfaces exposed to the incident electron beam (including all the slit system), has been measured to be less than 10^{-5} of the incident beam intensity. The contribution to the present measurements, of elastically scattered electrons at low energies has been estimated to be less than 0.1%.

Other possible sources of systematic error which cause the strong forward peak have been considered and no effect found: the pressure effect on the incident beam intensity; the sensitivity of the channeltron multiplier to the background pressure.

The DDCS of secondary electrons with 100- and 200-eV incident energies have a shape and trend similar to that of 50-eV incident energy.

Figure 2 shows a three-dimensional-perspective diagram of DDCS of secondary electrons at

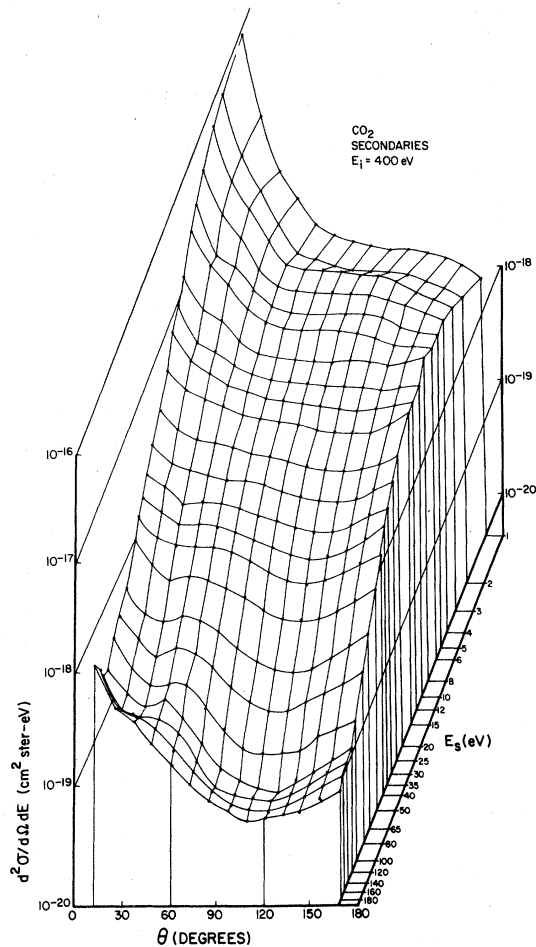


FIG. 2. Three-dimensional-perspective diagram of secondary electrons ejected from CO_2 by 400-eV electron impact.

400-eV incident energy. For secondary energies less than 10 eV the distribution tends to be isotropic above 60° with a strong forward scattering at angles less than 60° . A secondary maximum in the distribution near 60° begins to appear for energies above 30 eV. This peak is due to the conservation of energy and momentum of the colliding system ($\text{CO}_2 + e$). The peak is not clearly observable for secondary electron energies less than 30 eV at any of the incident energies used. This peak is observed for the 200-eV incident energy, but not all for 50- and 100-eV incident energies.

Figure 3 shows a typical DDCS of secondary electrons at a secondary electron energy of 30 eV for a 400-eV incident energy along with the results of Opal *et al.*⁸ for 500-eV incident energy. The result of Opal *et al.* agrees neither in shape nor in magnitude with the present result. The

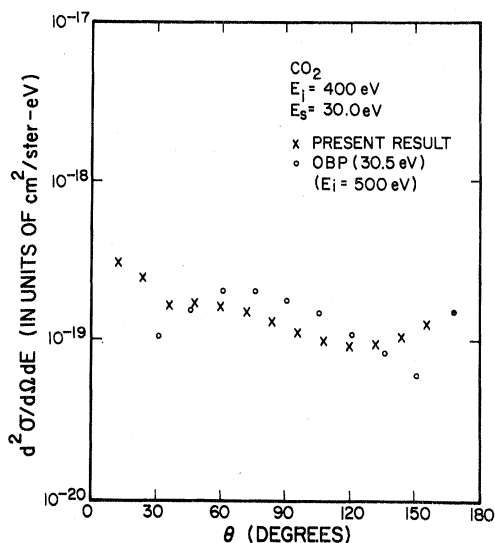


FIG. 3. DDCS, $d^2\sigma/d\Omega dE$, of secondary electrons ejected from CO₂ by 400-eV electron impact with 30-eV secondary electron energy. OPB is data of Opal *et al.* (Ref. 6) at 500-eV incident.

DDCS near 90° at 500-eV incident energy is larger than the present result by 35%. It is expected to be less than the value near 90° at 400-eV incident. The shape of DDCS of Opal *et al.* has a smaller scattering for the extreme angles than the present results in spite of the larger scattering near 90°. This may be partly due to the overcorrection of the data points in their measurements, i.e., their data points were corrected as in a volume experiment (static gas experiment) even though a crossed-beam method was used. It is also noted that the present measurements have an acceptance angle less than 4° in the detector system compared to that of Opal *et al.*, which was 15°.

Figure 4 shows a singly differential cross section (SDCS) at 400-eV incident energy along with the result of Opal *et al.*⁶ at 500-eV incident energy. There is a good agreement in shape between the present results and those of Opal *et al.*⁶ However, the magnitude of SDCS for a 500-eV incident beam is expected to be smaller than that of a 400-eV incident beam. It is noted that there is a peak near 2–3 eV due to an autoionization state of CO₂. This peak appears for the four incident energies studied.

Figure 5 shows a total ionization cross section of CO₂ by electron impact (which includes all the dissociative ionization cross section) along with the results of Rapp and Englander-Golden¹ and those of Crowe and McConkey.² The results of Crowe and McConkey were the pure direct single

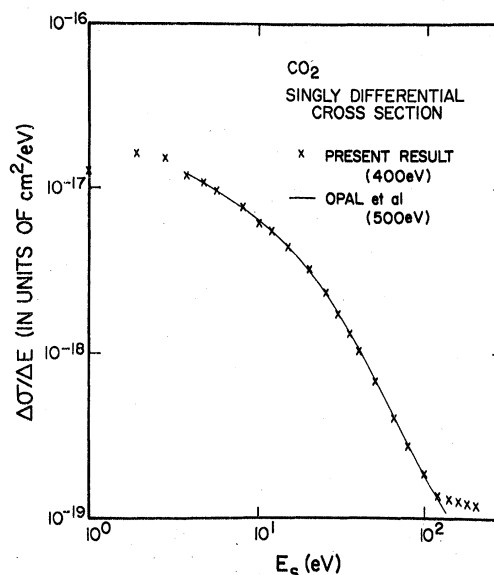


FIG. 4. SDCS, $\Delta\sigma/\Delta E$, of secondary electrons ejected from CO₂ by 400-eV electron impact along with the results of Opal *et al.* (Ref. 6) at 500-eV electron impact.

ionization cross section. The difference between the present results and those of Crowe and McConkey shows mainly the contribution from the dissociative ionizations. Typically, the contribution of the dissociative ionization is estimated to be 33% of the direct ionization cross section at 100-eV incident energy. Also it is interesting to note that the maximum contribution from the dissociative ionization is near 100-eV incident energy and becomes smaller as the incident energy increases or decreases from 100 eV.

Finally, Fig. 6 shows a Platzman plot for four

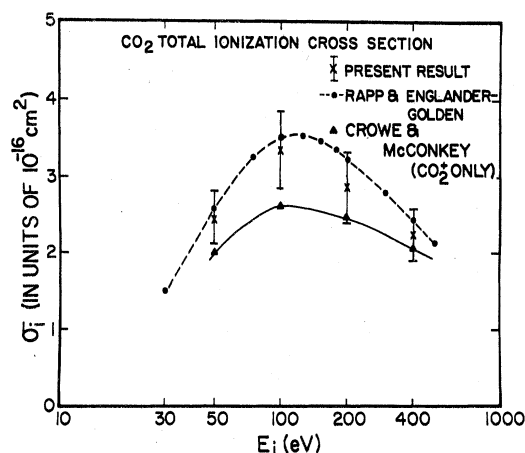


FIG. 5. Total ionization cross section of CO₂ by electron impact along with the results of Rapp and Englander-Golden (Ref. 7) and of Crowe and McConkey (Ref. 2).

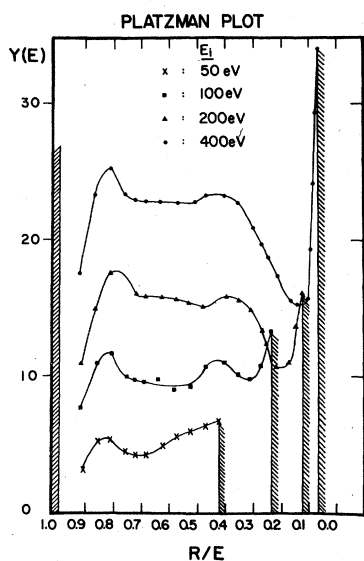


FIG. 6. Platzman plot of secondary electrons ejected from CO_2 by 50-, 100-, 200-, and 400-eV electron impact.

incident energies. The Platzman plot checks the consistency of the experimental data on secondary electrons by a plot of the ratio $Y(E)$ of the measured SDCS to the Rutherford cross section per electron as a function of the inverse of the energy transfer R/E of the incident electron to the target particle (R is the Rydberg constant and E is the sum of ionization and secondary electron energy). The shape of the energy distribution for slow secondary electrons in the Platzman plot resembles the shape of the corresponding photoionization cross section. A detailed discussion of the plot can be found elsewhere.¹⁰ There is an obvious peak in the plot representing an autoionization process for all incident energies near 2.5-eV ($R/E \approx 0.83$) secondary electron energy. This peak

also was shown in photoionization cross sections measured by Nakata *et al.*¹¹ near the 760-Å wavelength.

IV. SUMMARY

This paper presents the results of doubly differential cross section measurements of secondary electrons ejected from CO_2 by electron impact utilizing a crossed-beam method. The incident energies used were 50, 100, 200, and 400 eV. The energy and angular range of the secondary electrons measured were from one-half the difference between the incident energy and ionization potential to 1.0 eV and from 12° to 156° , respectively. The resultant uncertainty of the present results is less than $\pm 17\%$ except for low secondary energies ($\pm 26\%$).

The present results show a strong forward peak in the DDCS of all secondary electrons for all incident energies and an autoionization peak in the singly differential cross section near 2.4 eV.

There is a good agreement in shape between the present results at 400-eV incident energy and those of Opal *et al.*⁶ at 500-eV incident in singly differential cross sections. Significant differences have been found between the doubly differential cross sections reported here and those of Opal *et al.*⁶

ACKNOWLEDGMENT

This work is supported by National Science Foundation, Atmospheric Research Section, NSF Grant No. ATM77-27215. The authors are grateful to Dr. Y.-K. Kim at Argonne National Laboratory for many valuable discussions, especially, in theoretical part throughout this work. Also authors thank C. H. Kuo for his assistance in taking and analyzing the data.

¹D. Rapp and P. Englander-Golden, *J. Chem. Phys.* **43**, 1464 (1965).

²A. Crowe and J. W. McConkey, *J. Phys. B* **7**, 349 (1974).

³T. D. Märk and E. Hille, *J. Chem. Phys.* **69**, 2492 (1978).

⁴J. Peresse and F. Tuffin, *Methodes Phys. Anal.* **3** (1967).

⁵B. Adamczyk, A. J. H. Boerboom, and M. Lukasiewicz, *Int. J. Mass Spectrom. Ion Phys.* **9**, 407 (1972).

⁶C. B. Opal, E. C. Beaty, and W. K. Peterson, *At. Data*

4, 209 (1972).

⁷T. W. Shyn and W. E. Sharp, *Phys. Rev. A* **19**, 557, (1979).

⁸T. W. Shyn, R. S. Stolarski, and G. R. Carignan, *Phys. Rev. A* **6**, 1002 (1972).

⁹T. W. Shyn, W. E. Sharp, and G. R. Carignan, *Phys. Rev. A* **17**, 1855 (1978).

¹⁰Y.-K. Kim, *Radiat. Res.* **61**, 21 (1975); **64**, 96 (1975); **64**, 205 (1975).

¹¹R. S. Nakata, K. Watanabe, and E. M. Matsunaga, *Science of Light (Tokyo)* **11**, 54 (1965).